Human Aldose Reductase: Subtle Effects Revealed by Rapid Kinetic Studies of the C298A Mutant Enzyme†

Charles E. Grimshaw,*,‡ Kurt M. Bohren,§ Chung-Jeng Lai,‡ and Kenneth H. Gabbay§

Whittier Diabetes Program, Department of Medicine, University of California, San Diego, La Jolla, California 92093-0983, and Molecular Diabetes and Metabolism Section, Departments of Pediatrics and Cell Biology, Baylor College of Medicine, Houston, Texas 77030

Received March 13, 1995; Revised Manuscript Received July 24, 1995⊗

ABSTRACT: Transient kinetic data for D-xylose reduction with NADPH and NADPD and for xylitol oxidation with $NADP^+$ catalyzed by recombinant C298A mutant human aldose reductase at pH 8 have been used to obtain estimates for each of the rate constants in the complete reaction mechanism as outlined for the wild-type enzyme in the preceding paper (Grimshaw et al., 1995a). Analysis of the resulting kinetic model shows that the nearly 9-fold increase in V_{xylose}/E_t for C298A mutant enzyme relative to wild-type human aldose reductase is due entirely to an 8.7-fold increase in the rate constant for the conformational change that converts the tight ($K_{i\ NADP^+} = 0.14\ \mu M$) binary *E·$NADP^+$ complex to the weak ($K_{d\ NADP^+} = 6.8\ \mu M$) E·$NADP^+$ complex from which $NADP^+$ is released. Evaluation of the rate expressions derived from the kinetic model for the various steady-state kinetic parameters reveals that the 37-fold increase in K_{xylose} seen for C298A relative to wild-type aldose reductase is largely due to this same increase in the net rate of $NADP^+$ release; the rate constant for xylose binding accounts for only a factor of 5.5. A similar 17-fold increase in the rate constant for the conformational change preceding NADPH release does not, however, result in any increase in $V_{xylitol}/E_t$, because hydride transfer is largely rate-limiting for reaction in this direction. By contrast, the rate constant for conformational clamping in the opposite direction (weak → tight binary complex) is not greatly affected by the mutation, suggesting that Cys298 does not regulate the rate of closure of the nucleotide enfolding protein loop, but does stabilize the closed conformation. The rate of hydride transfer is reduced 2-fold in the C298A mutant, which, when combined with the increase in V_{xylose}/E_t, results in a small, but significant, primary deuterium isotope effect on turnover ($^DV_{xylose} = 1.07$). These results demonstrate the utility of using the kinetic model developed for the wild-type enzyme to analyze transient kinetic data in order to ascribe changes in kinetic parameters (V/E_t, K_m, ^DV, etc.) to changes in individual rate constants in the overall mechanism.

Cysteine 298 appears to be a key residue in defining the unique properties of aldose reductase (AR)[1] as a member of the broader NADP-dependent aldo−keto reductase superfamily. Unlike the important active site residues which have been shown to participate in the catalytic mechanism, including Tyr48, Lys77, Asp43, and possibly His110 (Tarle et al., 1993; Bohren et al., 1994), Cys298 is not strictly conserved among the members of this enzyme superfamily (Qin & Cheng, 1994; Bruce et al., 1994). Yet, chemical modification of this residue can lead to pronounced changes in the kinetic properties of AR, most often expressed as an increase in V/E_t for aldehyde reduction, and a much larger increase in the K_m for the aldehyde substrate, such that $V/K_{aldehyde}E_t$ shows a net decrease (Petrash et al., 1992, 1993; Bohren & Gabbay, 1993; Bhatnagar et al., 1994). Modification of Cys298 can also result in a pronounced loss of binding affinity for some, but not all, compounds developed as potential aldose reductase inhibitors (ARIs) for the prevention and treatment of diabetic complications (Vander Jagt & Hunsaker, 1993; Bhatnagar et al., 1994), a factor which may be important in predicting the success of ARI therapy *in vivo*.

Cys298 has been the target of site-directed mutagenesis studies aimed at establishing structure−function relationships for hAR. Studies in which Cys298 was converted to a serine residue (C298S mutant) showed that this residue is not an essential component of the catalytic machinery (Petrash et al., 1992, 1993; Bhatnagar et al., 1994) and further established that Cys298 is the residue involved in the formation of "oxidized" or "activated" enzyme forms (Bohren & Gabbay, 1993). However, the kinetic properties of the C298S mutant enzyme are clearly distinct from those of the oxidized enzyme form, since the latter shows no increase in V/E_t for aldehyde reduction and a much larger decrease in ARI binding affinity (Vander Jagt & Hunsaker, 1993; Grimshaw & Lai, 1995). Unfortunately, our understanding of these subtle kinetic and mechanistic effects has until now been limited to a discussion of the observable kinetic parameters, e.g., V/E_t, K_m, $^DV/K$, and so forth, with no reliable means to assign an observed change to a specific step or

† This work was supported by NIH Grants DK 43595 (C.E.G.) and EY 11018 (K.H.G.), Juvenile Diabetes Foundation grants (K.M.B. and K.H.G.), and the Harry B. and Aileen B. Gordon Foundation (K.H.G.).

* Address correspondence to this author, at the University of California, San Diego, Whittier Diabetes Program, Department of Medicine 0983, 9500 Gilman Dr., La Jolla, California 92093-0983. Phone: (619) 535-8037 or (619) 622-8422 (new); Fax: (619) 535-0894; Internet: cgrimshw@scripps.edu.

‡ University of California, San Diego.

§ Baylor College of Medicine.

⊗ Abstract published in *Advance ACS Abstracts,* October 15, 1995.

[1] Abbreviations: Na_2EDTA, disodium ethylenediaminetetraacetate; $NADP^+$, β-nicotinamide adenine dinucleotide phosphate; NADPH, reduced form of $NADP^+$; AR, aldose reductase; hAR, recombinant human aldose reductase; NADPD, (4*R*)-[4-$^2H_2$]NADPH; DTT, dithiothreitol; LADH, liver alcohol dehydrogenase; LDH, lactate dehydrogenase; ARI, aldose reductase inhibitor.

0006-2960/95/0434-14366$09.00/0

steps in the reaction mechanism. The use of stopped-flow kinetic methods combined with a complete kinetic model for wild-type hAR, presented in the preceding paper (Grimshaw et al., 1995a), now provides us with that ability.

The Cys298Ala mutant was originally developed as one of many mutants designed to identify the cysteine residue responsible for the thiol sensitivity of the aldose reductase enzyme (Bohren & Gabbay, 1993). The thiol sensitivity of the purified enzyme is reflected in the partially oxidized enzyme forms which are generated either during purification or storage of the enzyme (Vander Jagt et al., 1988, 1990; Grimshaw et al., 1989; Bhatnagar et al., 1989; Liu et al., 1989; Robinson et al., 1994; Cappiello et al., 1994). Preliminary studies of C298A mutant hAR showed that some properties were similar to the C298S enzyme, but some were quite different. Thus, C298A displayed an increase in V/E_t for aldehyde reduction and a larger increase in the $K_{aldehyde}$ value, similar to the changes noted for the C298S mutant. However, unlike the C298S mutant, K_i values for inhibition by various ARIs were comparable for C298A mutant and wild-type enzyme.

In this study, we present pre-steady-state transient kinetic data to support the assignment of each of the rate constants for C298A mutant hAR, based on the kinetic model developed for the wild-type enzyme in the preceding paper (Grimshaw et al., 1995a). The results will show that the primary effect of the cysteine → alanine substitution is to alter the rate of the conformational change that allows relaxation of the tight binary E·nucleotide complex to the more weakly bound complex, from which the nucleotides can dissociate. As we have shown for the wild-type enzyme, this conformational "clamping" appears to be a key to hAR's catalytic prowess as a broad-specificity aldehyde reducing catalyst. Smaller, but significant, changes are also ascribed to the rate of aldehyde binding and of hydride transfer at the ternary complex stage of the reaction mechanism. Thus, the changes in the observable kinetic parameters can in each instance be directly correlated with changes in the individual rate constants using the kinetic model. The procedure described here should prove valuable for the detailed kinetic and mechanistic interpretation of other mutants of this important class of NAD(P)H-dependent aldo−keto reductases.

MATERIALS AND METHODS

The mutant C298A human aldose reductase construct was prepared by oligo-directed mutagenesis, and the enzyme was overexpressed in *Escherichia coli* and purified essentially as described (Bohren et al., 1991). Enzyme was stripped of all nucleotide using the method of Ehrig et al. (1994), and the protein concentration was estimated using $\epsilon^{280\,nm} = 48.2$ mM^{-1} cm^{-1}. All other chemicals and methods were as described for the studies of the wild-type enzyme (Grimshaw et al., 1995a).

RESULTS

Nucleotide Binding. Progress curves (quenching of enzyme fluorescence) for nucleotide binding to C298A mutant hAR were in all cases best fit using a single exponential (Figure 1). Unlike the wild-type enzyme, we saw no evidence with the C298A mutant enzyme for a second slower phase using either $NADP^+$ or NADPH over a wide range of

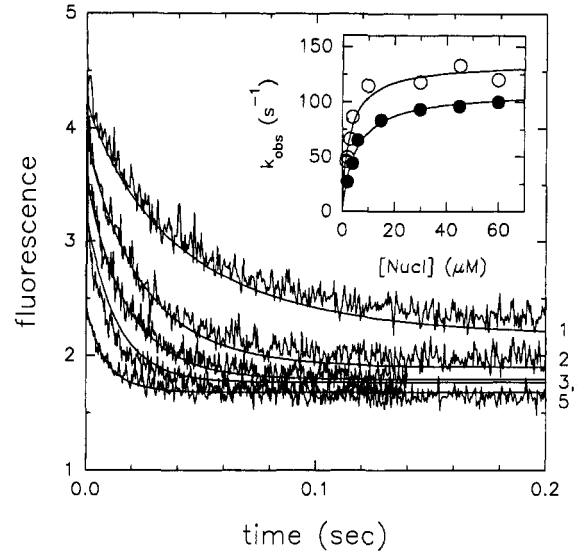

FIGURE 1: Stopped-flow progress curves for $NADP^+$ binding to C298A mutant hAR monitored as quenching of enzyme fluorescence ($_{294\,nm}F_{>315\,nm}$). Reactions in standard phosphate buffer contained 1.5 μM enzyme and the following concentrations of $NADP^+$: 2 μM (1); 4 μM (2); 6 μM (3); 10 μM (4); and 45 μM (5). Actual progress curves shown are averages of 3−4 kinetic transients; solid lines were calculated using rate constants (Table 1) determined for a two-step binding mechanism by KINSIM/FITSIM analysis of the entire data set for each nucleotide. First-order rate constants (k_{obs}) determined from Bio-Kine analysis of individual progress curves showed standard errors of 1% or better. Inset: Plots of k_{obs} versus nucleotide concentration with NADPH (●) and $NADP^+$ (○) show saturation kinetics; solid lines were calculated from fits of the k_{obs} data as described in Results.

Scheme 1

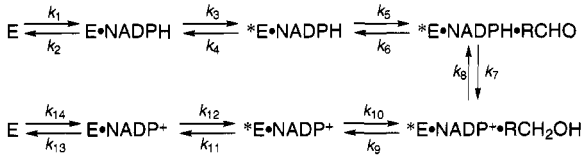

nucleotide concentration. This observation is consistent with the idea that partial oxidation at Cys298 is primarily responsible for the biphasic nucleotide binding kinetic data reported by others (Kubiseski et al., 1992). Plots of k_{obs} versus nucleotide concentration ([nucleotide]) displayed saturation behavior (inset, Figure 1), consistent with a two-step binding mechanism (k_1-k_4 (NADPH) or $k_{14}-k_{11}$ ($NADP^+$)) as detailed in Scheme 1 for wild-type enzyme in the preceding paper (Grimshaw et al., 1995a), where E is C298A mutant hAR, RCHO is D-xylose, RCH_2OH is xylitol, and *E is the isomerized form of the enzyme. Similar to the procedure used for the wild-type enzyme, data for k_{obs} as a function of nucleotide concentration were fitted either using a simple equation describing the two-step binding mechanism or using least-squares analysis of the progress curves themselves by the KINSIM/FITSIM software package to obtain estimates for each of the rate constants. As shown in Table 1, the derived values routinely displayed standard errors less than 20%, and the values obtained by the two different fitting procedures were in reasonable agreement. In general, the weak initial E·NADP(H) complexes of the C298A mutant enzyme displayed K_d values only 2-fold higher than those estimated for the wild-type enzyme. However, the extent of "clamping" to form the tight *E·NADP(H) complex, as reflected by the ratio of initial K_d to

Table 1: Rate and Equilibrium Constants for Nucleotide Binding to C298A Mutant hAR

nucleotide	fitting method	K_d (μM)	k_1 (M^{-1} s^{-1})	k_2 (s^{-1})	k_3 (s^{-1})	k_4[a] (s^{-1})	K_i[b] (nM)	K_d/K_i
$NADP^+$	SigmaPlot	2.7 ± 2.3			102 ± 30	⟨0.9⟩	24	114
	Fitsim	6.8	(2.5 ± 0.1) × 10^8	1700 ± 90	100 ± 4	2.0 ± 0.1	138	49
NADPH	SigmaPlot	3.2 ± 1.4			150 ± 17	⟨0.12⟩	270	12
	Fitsim	2.8	(1.7 ± 0.1) × 10^8	470 ± 40	90 ± 3	14 ± 0.2	430	6.5

[a] Broken brackets contain steady-state $\langle V/E_t \rangle$ values for reaction in the opposite direction. [b] $K_i = k_2/k_1(1.0 + (k_3/k_4))$ is the dissociation constant for the tight *E·$NADP^+$ complex; the corresponding rate constants from Scheme 1 should be substituted for NADPH, with k_{14}–k_{11} (NADPH) equivalent to k_1–k_4 ($NADP^+$).

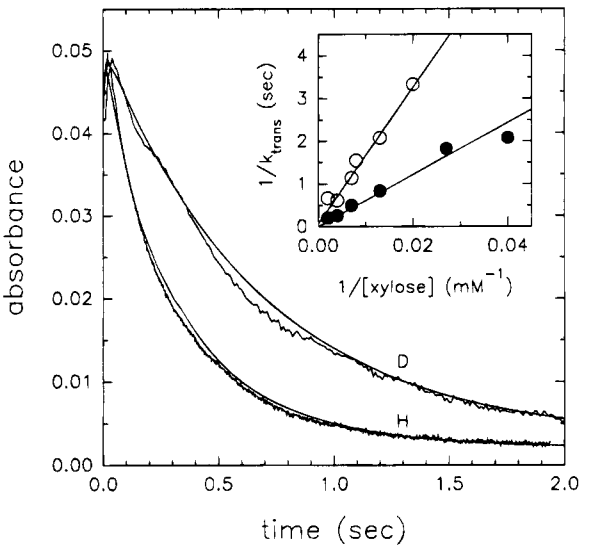

FIGURE 2: Single turnover stopped-flow progress curves for C298A mutant hAR-catalyzed D-xylose reduction monitored by absorbance change at 363 nm. Reactions in standard phosphate buffer contained 12.5 μM enzyme, 250 mM D-xylose, and 11.5 μM NADPH (H) or NADPD (D). Actual progress curves are shown; solid lines were calculated using rate constants determined for the complete kinetic mechanism (Scheme 1) by KINSIM/FITSIM analysis of the entire data set including progress curves determined for each nucleotide at a range of D-xylose concentrations. First-order rate constants (k_{trans}) determined from Bio-Kine analysis of the $A_{363\,nm}$ decrease for individual progress curves showed standard errors of 6% or better. Inset: Only slope values (K_{xylose}/k_{trans}) were determined from double-reciprocal plots of $1/k_{trans}$ versus 1/[xylose] for NADPH (●) and NADPD (○) since the intercepts were not significantly different from zero.

final K_i value, was about 13- to 16-fold less for the C298A mutant enzyme. This fact will become important in the discussion of the kinetic effects on turnover resulting from mutation of Cys298 to an alanine residue.

Single Turnover Experiments. Figure 2 shows a representative pair of progress curves measured using NADPH and NADPD at 250 mM D-xylose. Such progress curves routinely displayed an increase in $A_{363\,nm}$ during the first 30–50 ms due to the shift in absorbance maximum for bound NADPH, followed by a decrease in absorbance due to NADPH oxidation. The latter decrease in $A_{363\,nm}$ was in all cases best fit using a single exponential. When the experimentally determined first-order rate constant (k_{trans}) was plotted in double-reciprocal fashion as $1/k_{trans}$ versus 1/[D-xylose] with either NADPH or NADPD, the line appeared to pass through the origin (inset, Figure 2). A fit of these data to:

$$k = k_{max}A/(K_{1/2} + A) \quad (1)$$

where k_{max} is the maximum value of k, A is the concentration of substrate (D-xylose), and $K_{1/2}$ is the apparent half-saturation constant for A, confirmed that the k_{max} values were not well determined. The problem occurs because the K_{xylose} value for xylose in a single turnover experiment, as estimated from the kinetic model,[2] is 1.75 M. This value is far greater than the maximum D-xylose concentration used (545 mM), and thus we were unable to saturate the transient reaction in order to obtain a statistically significant value for k_{trans}. Fitting the data in double-reciprocal form to a straight line and assuming an intercept value equal to zero, however, gave good values for the slopes (equal to k_{trans}/K_{xylose}) of 20 ± 3 M^{-1} s^{-1} for NADPH and 7.9 ± 3.0 M^{-1} s^{-1} for NADPD. These data confirm that, similar to wild-type hAR, there is a large primary deuterium isotope effect[3] on the single turnover transient ($^Dk_{trans}/K_{1/2}$ = 2.5 ± 1.0), indicating that hydride transfer makes a significant contribution to the overall rate limitation of the single turnover transient.

Multiple Turnover ("Burst Kinetics") Experiments. When the NADPH concentration was increased to 140 μM to allow multiple turnovers, progress curves displayed "burst kinetics" with an initial exponential decline in absorbance followed by a steady-state rate of NADPH disappearance (Figure 3). However, the magnitude of the "burst" was much lower than for wild-type enzyme (see below). As a result, progress curve analysis using the Bio-Kine software only yielded accurate values for k_{ss} as a function of D-xylose concentration. Fitting these data for the steady-state rate (k_{ss}) to eq 1 gave the following results for NADPH, k_{ss} = 2.1 ± 0.1 s^{-1} (equal to V_{xylose}/E_t) and K_{xylose} = 73 ± 13 mM (equal to K_{xylose}), while for NADPD, k_{ss} = 1.9 ± 0.3 s^{-1} and K_{xylose} = 165 ± 50 mM. The calculated primary deuterium isotope effects on k_{ss} and k_{ss}/K_{xylose} derived from these data are compared in Table 2 with the corresponding value determined from the single turnover experiments ($^D(k_{trans}/K_{xylose})$), and with those determined by the conventional method of direct comparison of initial velocities ($^DV_{xylose}$ and $^DV/K_{xylose}$). As we saw for the wild-type enzyme, multiple turnover progress curves for xylitol oxidation with $NADP^+$ displayed only a steady-state phase as shown by a linear appearance of NADPH absorbance with time (not shown). Fitting the k_{ss} data as a function of xylitol concentration to eq 1 gave k_{ss} = 0.13 ± 0.01 s^{-1} (equal to $V_{xylitol}/E_t$) and $K_{xylitol}$ = 340 ± 60 mM (equal to $K_{xylitol}$).

The set of progress curves for both single turnover and multiple turnover experiments for reduction of D-xylose with

[2] K_{xylose} estimated as $(k_{eff} + k_6)/k_5$, where $k_{eff} = [(1/k_7) + (1/k_3)]^{-1}$ is the effective rate constant for a single turnover transient at infinite xylose concentration according to Scheme 1.

[3] The isotope effect nomenclature used is that of Northrop (1977) and Cleland (1987) in which a leading superscript indicates the isotope effect being studied. Thus, ^DV, $^DV/K$, and ^Dk are primary deuterium isotope effects on V/E_t, V/KE_t, and k, respectively.

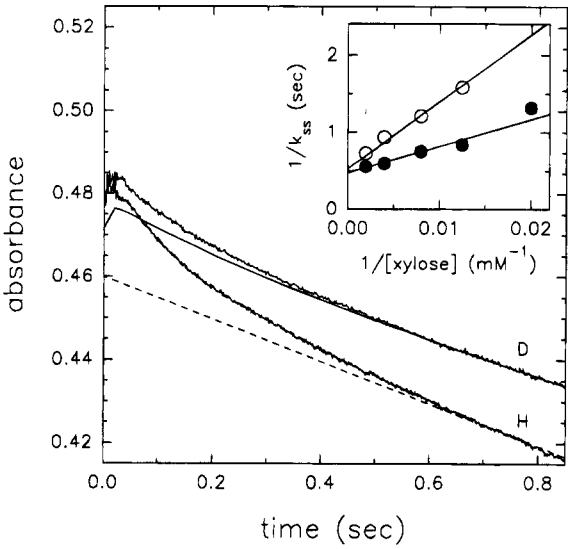

FIGURE 3: Multiple turnover stopped-flow progress curves for C298A mutant hAR-catalyzed D-xylose reduction. Reactions in standard phosphate buffer contained 12.5 μM enzyme, 250 mM D-xylose, and 140 μM NADPH (H) or NADPD (D). Actual progress curves shown emphasize the pre-steady-state burst; data were collected up to 10 s to establish the steady-state rate. The solid lines were calculated as described for Figure 2. The burst magnitude (-0.0250 ± 0.010 $A_{363\,nm}$) for NADPH (dashed line) corresponds to 0.59 enzyme equivalents. Inset: Double-reciprocal plots of $1/k_{ss}$ versus 1/[xylose] for NADPH (●) and NADPD (○) show saturation kinetics for the linear, steady-state phase of the reaction.

Table 2: Comparison of Calculated and Observed Deuterium Isotope Effects for C298A Mutant hAR

measurement[a]	$^{D}k_{max}$	$^{D}(k_{max}/K_{xylose})$
single turnover (k_{trans})	—[c]	2.5 ± 1.0
burst: k_{burst} calcd from model[b]	4.09	2.65
stopped-flow steady state (k_{ss})	1.10 ± 0.10	2.5 ± 1.0
initial velocity (V_{xylose}/E_t)	1.07 ± 0.02	2.70 ± 0.09
calcd "intrinsic" effect: $^{D}k_7 = (k_{7H}/k_{7D})$	6.50	

[a] All measurements in 33 mM phosphate buffer (pH 8.0) at 25 °C. [b] At saturating levels of NADPH and xylose, $k_{burst} = ((1/k_3) + (1/k_7))^{-1}$; thus, $^{D}k_{burst} = (k_{burstH}/k_{burstD}) = (^{D}k_7 + (k_{7H}/k_3))/(1.0 + (k_{7H}/k_3)) = (6.50 + 0.78)/(1.00 + 0.78) = 4.09$. At limiting [D-xylose], $^{D}(k_{burst}/K_{xylose}) = (^{D}k_7 + (k_{7H}/k_6))/(1.0 + (k_{7H}/k_6)) = 2.65$. [c] Not able to determine accurately since the maximum D-xylose concentration (545 mM) is much less than the apparent K_{xylose} (1.75 M).

NADPH and NADPD was analyzed using the KINSIM and FITSIM software according to the complete reaction mechanism outlined in Scheme 1. As for the wild-type enzyme, analyses of the various sets of progress curves were used to refine the values for k_5-k_8, using both single turnover and multiple turnover experiments with either NADPH or NADPD. These simulations proved to be insensitive to large changes in the values of k_9 and k_{10}. These rate constants were thus set at values high enough to be kinetically transparent, yet maintain a ratio (k_9/k_{10}) equal to the $K_{xylitol}$ value determined either by conventional steady-state kinetic methods or from the saturation kinetics observed for the linear phase of xylitol oxidation in multiple turnover experiments. The value of k_8 was limited to a narrow range by the $V_{xylitol}/E_t$ value determined for xylitol oxidation, and by the fact that the net rate corresponding to k_8 is at least 100-fold slower than any other step for reaction in this direction. However, as for the wild-type enzyme, because only one data set contributes significantly to the assignment of this

Table 3: Estimated Rate Constants for the Reactions of D-Xylose and Xylitol[a]

	forward		reverse
k_1	1.7×10^8 M^{-1} s^{-1}	k_2	470 s^{-1}
k_3	90 s^{-1}	k_4	14 s^{-1}
k_5	40 M^{-1} s^{-1} [c]	k_6	30 s^{-1}
k_7	70 s^{-1} (11 s^{-1})[b]	k_8	0.33 s^{-1} (0.05 s^{-1})[b]
k_9	1.6×10^6 s^{-1}	k_{10}	5×10^6 M^{-1} s^{-1}
k_{11}	2.0 s^{-1}	k_{12}	100 s^{-1}
k_{13}	1700 s^{-1}	k_{14}	2.5×10^8 M^{-1} s^{-1}

[a] Rate constants for the binding of NADPH (k_1-k_4) and of $NADP^+$ ($k_{11}-k_{14}$) were estimated by progress curve analysis and were fixed in all simulations. The ratio of k_9 to k_{10} was fixed at 0.32 M, equal to the $K_{xylitol}$ value. Eight progress curves, four forward and four reverse reactions, were used for these simulations. Standard errors were 20% or better. [b] Values given in parentheses are for NADPD. Actual progress curves were used to estimate k_{7D}, while k_{8D} was calculated as $k_{8D} = k_{8H}{}^{D}K_{eq}/{}^{D}k_7$ (see text for details). The values of k_5-k_7 provided the best overall fits for both the NADPH and NADPD progress curve data sets. [c] When the xylose concentration is corrected for the 0.02% level of free carbonyl form (Hayward & Angyal, 1977), $k_5 = 2 \times 10^5$ M^{-1} s^{-1}.

Table 4: Comparison of Calculated and Measured Kinetic Parameters for C298A Mutant hAR

parameter	calcd	measured[a]
V_{xylose}/E_t (s^{-1})	1.8	1.7 ± 0.1
K_{NADPH} (μM)	0.066	0.15 ± 0.02
K_{xylose} (mM)	74	56 ± 5
$K_{i\,NADPH}$ (μM)	0.43	0.03[b]
$K_{d\,NADPH}$ (μM)	2.8	
$V_{xylitol}/E_t$ (s^{-1})	0.10	0.12 ± 0.01
K_{NADP^-} (μM)	0.007	<0.10
$K_{xylitol}$ (mM)	320	280 ± 30
$K_{i\,NADP^-}$ (μM)	0.14	0.06[b]
$K_{d\,NADP^+}$ (μM)	6.8	

[a] Determined from initial velocity studies in 33 mM phosphate buffer (pH 8.0) at 25 °C. [b] Determined by fluorescence titration in 5 mM phosphate buffer (pH 7.0) at 20 °C (Ehrig et al., 1994).

rate constant, the absolute magnitude of k_8 must be considered approximate at this point. The k_{8D} value was estimated as $k_{8D} = (k_{8H}{}^{D}K_{eq}/{}^{D}k_7)$, where $^{D}k_7 = k_{7H}/k_{7D}$ is determined directly from progress curves with NADPH and NADPD and $^{D}K_{eq} = (k_{7H}/k_{8H})/(k_{7D}/k_{8D})$ is the equilibrium isotope effect for NAD(P)D-linked reduction of an aldehyde to a primary alcohol, $^{D}K_{eq} = 0.93$ (Cook et al., 1980). Table 3 contains a list of the estimated rate constants determined for the mechanism shown in Scheme 1.

Values of the observable kinetic parameters (e.g., V_{xylose}/E_t, K_{xylose}, etc.) were also calculated by substituting the estimated rate constants from Table 3 into kinetic expressions derived according to Scheme 1 (see supporting information in Grimshaw et al., 1995a). As shown in Table 4, the agreement between the measured and calculated values is quite good. As a further check on the internal consistency of the proposed kinetic model, the calculated K_{eq} value (1.4×10^{13} M^{-1}, based on the free carbonyl form of D-xylose (Hayward & Angyal, 1977)) was found to be in fair agreement with the published values (average value of 5.2×10^{13} M^{-1}, based on free carbonyl form) for reduction of the α-hydroxyaldehydes, DL-glyceraldehyde (Kormann et al., 1972), and D-xylose (Moonsammy & Stewart, 1961).

Magnitude of the Pre-Steady-State Burst. The size of the pre-steady-state burst is determined by (1) the relative rates for the sequence of steps (including hydride transfer) that

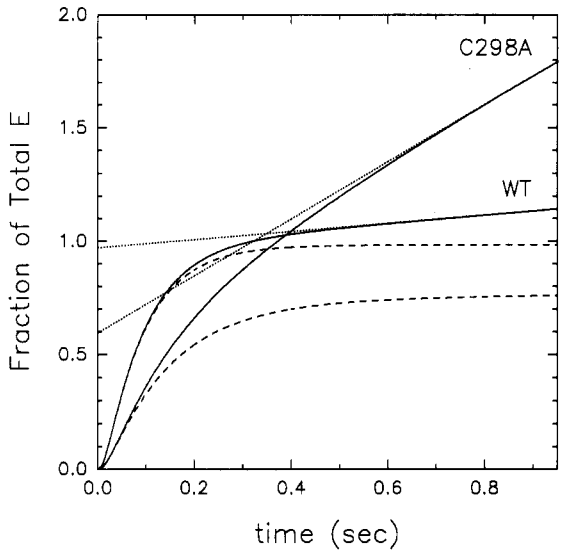

FIGURE 4: KINSIM simulation comparing the pre-steady-state burst for wild-type and C298A mutant hAR. KINSIM simulations generated using the estimated rate constants from the appropriate kinetic model show reaction progress curves for total $NADP^+$ production (solid line), formation of the steady-state level of *E·$NADP^+$ (dashed line), and the linear steady-state rate of $NADP^+$ production (dotted line). Extrapolation back to time zero shows that the "apparent" burst for the C298A mutant enzyme ($0.59E_t$) is much less than for wild-type enzyme ($0.97E_t$).

produce *E·$NADP^+$ and (2) the net rate for release of $NADP^+$ from *E·$NADP^+$. This is shown graphically in Figure 4 where we compare the simulated progress curves for D-xylose reduction with NADPH for wild-type and C298A mutant hAR at 75 and 250 mM D-xylose concentration, respectively. KINSIM was used along with estimated rate constants from the respective kinetic models for the two enzymes to simulate both total $NADP^+$ production and formation of the steady-state level of *E·$NADP^+$. The net rate for *E·$NADP^+$ production is largely fixed by $k_5' = k_5k_7$[D-xylose]$/(k_6 + k_7)$, because of the large apparent K_{xylose} values for wild-type (350 mM) and C298A mutant enzyme (1.75 M) for the pre-steady-state transient reaction. Thus, for wild-type enzyme $k_5' = 13.8\ s^{-1}$ and for C298A mutant enzyme $k_5' = 7.0\ s^{-1}$. The net rate constant (Cleland, 1975) for $NADP^+$ release, $k_{11}' = k_{11}k_{13}/(k_{12} + k_{13})$, is $0.19\ s^{-1}$ for wild-type and $1.9\ s^{-1}$ for C298A hAR, respectively. The fraction of E_t present as *E·$NADP^+$ during steady-state turnover ($f_{*E\cdot NADP^+} = $ *E·$NADP^+/E_t$) at a certain concentration of D-xylose is given by:

$$f_{*E\cdot NADP^+} = (1/k_{11}')[(1/k_5') + (1/k_{11}')] \qquad (2)$$

which is 0.98 for wild-type enzyme and 0.73 for C298A mutant enzyme. Finally, we must correct for rate of reaction during the linear steady-state phase, which when extrapolated back to time zero will effectively reduce the "apparent" burst from the actual $f_{*E\cdot NADP^+}$ value. This correction is approximately given by multiplying $0.693/k_5'$ (the $t_{1/2}$ corresponding to k_5') by the steady-state rate constant (k_{11}'). Thus, for wild-type enzyme the correction is quite small ($0.01E_t$), while for the C298A mutant enzyme the correction ($0.15E_t$) results in a net "apparent" burst of $0.73 - 0.15 = 0.58E_t$, which agrees quite well with the $0.59\ E_t$ burst observed experimentally at 250 mM D-xylose (Figure 3).

DISCUSSION

The utility of a kinetic model is a direct function of its ability to describe changes in the observable kinetic parameters (e.g., V/E_t, K_m, ^DV, etc.) in terms of individual rate constants in the mechanism, so these changes can ultimately be translated into structure–function relationships within the constraints of the enzyme's three-dimensional structure. Previous studies have shown that modification of the Cys298 residue in hAR, either by chemical (Del Corso et al., 1989; Liu et al., 1989, 1992a,b; Bhatnagar et al., 1989, 1994; Giannessi et al., 1993; Cappiello et al., 1994) or molecular biological means (Petrash et al., 1992, 1993; Bohren & Gabbay, 1993), results in enzyme forms displaying altered kinetic properties. Comparison of the results in Table 4 with the corresponding results from the preceding paper (Grimshaw et al., 1995a) shows that substitution of Cys298 with an alanine residue results in a nearly 9-fold increase in the forward rate of D-xylose reduction, a 37-fold increase in K_{xylose}, and a small, but significant increase in the deuterium isotope effects on both V_{xylose} and V/K_{xylose}. By applying the pre-steady-state kinetic data reported here to the kinetic model, we can now rationalize each of these changes in terms of the individual rate constants.

Analysis of the Kinetic Model. Inspection of Table 3 reveals that the major effect of the C298A mutation is on the rate constants (k_{11} and k_4) for the conformational change that opens the nucleotide enfolding loop and allows the release of $NADP^+$ in the forward, and of NADPH in the reverse, reaction, respectively. For reaction in the forward direction, the observed increase in V_{xylose}/E_t follows directly from the 8.7-fold increase in k_{11}, since this is the overall rate-limiting step. In the reverse reaction, the 17-fold increase in k_4 does not translate into a corresponding increase in $V_{xylitol}/E_t$ because the rate of hydride transfer (k_8) is the slow step in the alcohol oxidation direction. Furthermore, because, as we have shown (Grimshaw et al., 1995a), $K_{xylose} \cong k_{11}/k_5$, it is the 8.7-fold increase in k_{11} that makes the major contribution to the 37-fold increase the apparent K_{xylose} value. Thus, the major effect on the K_{xylose} value for the C298A mutant arises from a change in the rate constant for a step which occurs at a point in the mechanism where neither aldehyde substrate nor alcohol product is involved!

The data in Table 1 indicate that the effect of the Cys298 → Ala mutation on the nucleotide-induced conformational change is almost totally one of stabilizing the tightly bound *E·NADP(H) conformation, since the rate constants for the loop closing reactions (k_{12} and k_3) are not affected by the mutation. The shift in equilibrium away from the tight complex in the C298A enzyme averages 15-fold, which corresponds to a difference of about 1.5 kcal/mol in free energy. According to Fersht (1988), this energy difference translates into the loss of roughly a single hydrogen bond between uncharged groups in the C298A versus the wild-type binary *E·NADP(H) complex, although the specific interactions involved remain to be identified. Formation of the weak initial E·NADP(H) complex also shows about a 2-fold increase in K_d value relative to the wild-type enzyme.

X-ray crystallographic studies show that the Cys298 sulfhydryl group is 4.1 Å from the nicotinamide C4-position of the bound cofactor in a number of E·$NADP^+$·anion complexes (Wilson et al., 1992; Harrison et al., 1994; Bohren et al., 1994). These crystallographic studies also show that

segments of the nucleotide enfolding loop are thoroughly disordered with high B factors. There appear to be several points where the loop is anchored by specific interactions, e.g., Asp216 which forms a salt link with Lys21. The interaction of the sulfhydryl group of Cys298 with the nucleotide enfolding loop and the nucleotide appears to be another key interaction (Gabbay et al., unpublished). The crystallographic data are thus consistent with the conclusion from our stopped-flow kinetic studies that modification of the Cys298 thiol group leads to a weaker interaction with the nucleotide enfolding loop.

The next largest effect of the C298A mutation is on the xylose binding step. As we saw for the nucleotide-induced conformational change, the reaction is affected in primarily one direction, in this case, a 5.5-fold decrease in k_5 relative to the wild-type enzyme. By contrast, k_6 is increased only slightly, with the net effect being that the C298A mutant is less efficient at binding D-xylose to form the productive *E·NADPH·xylose complex, but once formed, the off-rate for xylose dissociation is comparable for the two enzymes. A similar but smaller effect (ca. 2-fold) is seen for xylitol binding, although, given the uncertainty in the k_9 and k_{10} values, we cannot define their relative contributions to $K_{xylitol}$. The value for k_5, after correction for the 0.02% level of free carbonyl form for D-xylose in aqueous solution (Hayward & Angyal, 1977), is still only 2.0×10^5 M^{-1} s^{-1}, which is far below the predicted rate for a diffusion-controlled process (ca. 10^8 M^{-1} s^{-1}). Thus, k_5 must consist of a two-step sequence, analogous to what we have described for nucleotide binding:

$$*E{\cdot}NADPH + RCHO \underset{k_{24}}{\overset{k_{23}}{\rightleftharpoons}} *E{\cdot}NADPH{\cdot}RCHO \underset{k_{26}}{\overset{k_{25}}{\rightleftharpoons}} {}^{\diamond}E{\cdot}NADPH{\cdot}RCHO \quad (3)$$

where the first step, a rapid equilibrium binding of xylose to form the initial *E·NADPH·RCHO complex, is followed by an active site reorganization to yield the productive $^{\diamond}$E·NADPH·RCHO complex in which hydride transfer takes place. The observed 5.5-fold decrease in k_5 could thus reflect either a decrease in k_{25} or a net decrease in the $K_{eq} = (k_{23}/k_{24})$ for the rapid equilibrium binding step.

The stopped-flow data require that k_{25} for D-xylose reduction not be significantly slower than k_3 or k_7. Thus, if k_{25} were much slower than k_3 or k_7 (but still larger than k_{11}, to ensure that burst kinetics were observed), expression of the intrinsic isotope effect on k_7 would be reduced or eliminated. As we have shown for both the wild-type and C298A mutant enzymes, the stopped-flow data clearly display a substantial deuterium isotope effect on the burst phase of the reaction (Figures 2 and 3). The estimated value of $^{D}k_7 = k_{7H}/k_{7D} \cong 6.5$ is furthermore near the maximum expected for the intrinsic primary deuterium isotope effect on an NAD(P)H-dependent carbonyl reduction reaction (Scharschmidt et al., 1984). However, with the smaller substrate, DL-glyceraldehyde, there is evidence that the step corresponding to k_{25} does make an important kinetic contribution to the expression of the intrinsic deuterium isotope effect (Grimshaw et al., 1995b).

The rate constants for hydride transfer decrease almost 2-fold for the C298A mutant enzyme compared to the rate constants estimated for wild-type enzyme. As noted above, this decrease has almost no effect on $V_{aldehyde}/E_t$ since k_{11} is rate-limiting. In the reverse reaction, the net effect on $V_{xylitol}/E_t$ is also small, since the 2-fold decrease in k_8 is almost exactly offset by a change in the partitioning ratio (k_6/k_7) so the net rate constant $(k_8' = k_6k_8/(k_6 + k_7))$ is unchanged for wild-type and C298A mutant enzyme. It is difficult at this point to pinpoint what could be the cause of this 2-fold decrease in hydride transfer rate. As we have already noted, the Cys298 thiol group is in close proximity to the active site, although clearly not involved in the actual hydride transfer reaction itself. The case may simply be that the proper alignment of aldehyde substrate, key active site residues, and the dihydronicotinamide ring of NADPH cannot be achieved in the presence of a truncated Ala298 residue.

One key to the unique catalytic ability of hAR to efficiently reduce a broad range of aldehyde substrates appears to be the very tight binding of the nucleotide cofactors (Grimshaw, 1992). The molecular mechanism whereby this tight binding is translated into catalytic efficiency remains to be established. It is clear, however, that the presence of Cys298 stabilizes the proper configuration of the flexible loop which holds the nucleotide tightly bound in both the *E·NADPH and *E·NADPH·xylose complexes. Comparison of the crystallographic data for the open (Rondeau et al., 1992) and closed (Wilson et al., 1992, 1993; Harrison et al., 1994; Bohren et al., 1994) conformations of wild-type hAR confirms that alignment of this flexible protein loop affects the positioning of not only the nucleotide, but also the key active site residues. Thus, it is not surprising that hydride transfer itself is affected to a minor degree by the C298A mutation. What is surprising is that there is apparently little effect on the intrinsic isotope effect, although, given the precision of these rate constant estimates, it would be premature to argue about the relative symmetry of the transition state for hydride transfer between the wild-type and C298A mutant enzymes. Such discussion must await more precise determination of the intrinsic effects, such as can be obtained by the multiple isotope effect method of Hermes et al. (1982).

Deuterium Isotope Effects. The larger isotope effects on the observable kinetic parameters for the C298A mutant enzyme (Table 2), relative to what we see for the wild-type enzyme, can also be understood in reference to the same changes in rate constants already described. Of particular interest is the detection of a small but significant isotope effect on V_{xylose}/E_t. As we described for the wild-type enzyme (Grimshaw et al., 1995a), the commitment factor, that controls the extent to which the intrinsic isotope effect on hydride transfer ($^{D}k_7$) is expressed on V_{xylose}/E_t, is $C_{Vf} \cong k_{7H}/k_{11}$ in:

$$^{D}V_{xylose} = (^{D}k_7 + C_{Vf} + C_r{}^{D}K_{eq})/(1.0 + C_{Vf} + C_r) \quad (4)$$

Because k_7 has decreased nearly 2-fold and k_{11} has increased nearly 9-fold, the wild-type value of $C_{Vf} \cong 565$ falls to $C_{Vf} \cong 38$ for the C298A mutant enzyme. The estimated $^{D}V_{xylose}$ is thus 1.14, which is in good agreement with the experimental value of 1.07−1.10 (Table 2). For $^{D}V/K_{xylose}$ (also $^{D}(k_{trans}/K_{xylose})$) the key commitment factor is $C_f = (k_{7H}/k_6)$ in:

$$^{D}V/K_{xylose} = (^{D}k_7 + C_f + C_r{}^{D}K_{eq})/(1.0 + C_f + C_r) \quad (5)$$

Table 5: Comparison of C298A, C298S, and "Oxidized" with Wild-Type hAR[a]

parameter	C298A/WT ratio[b]	C298S/WT ratio[c]	"oxidized"/WT ratio[d]
$V_{aldehyde}/E_t$	8.7	3.5	1.0
$K_{aldehyde}$	37	55	55
$K_{i\ sorbinil}$	1	10	1000
k_{11}	8.7	3.5	1.0
k_5	5.5	15	55

[a] Comparison given as kinetic parameter ratio (enzyme/WT) where a ratio >1 indicates a larger value for the modified enzyme relative to wild-type hAR (WT). [b] This study. [c] Data from Petrash et al. (1992). [d] Data from Vander Jagt and Hunsaker (1993).

Similarly, because k_{7H} has decreased nearly 2-fold while k_6 remains constant, the $C_f = 5.2$ for wild-type enzyme falls to $C_f = 2.3$ for the C298A mutant enzyme, resulting in a calculated value of ${}^DV/K_{xylose} = 2.65$, again in excellent agreement with the experimental values determined by stopped-flow for both the burst phase (2.5 ± 1.0) and the linear phase (2.5 ± 1.0) of the reaction, and by conventional initial velocity methods (2.70 ± 0.09). Due to the slow rate of hydride transfer in the reverse reaction ($k_8 = 0.33\ s^{-1}$), the value for $C_r = k_{8H}/k_9 \cong 0$ is not a factor in either eq 4 or eq 5. The influence of the k_7/k_6 ratio, also referred to as the "stickiness" of the aldehyde substrate (Cleland, 1977), will become apparent in our discussion of pH profiles in the ensuing paper (Grimshaw et al., 1995b). Unfortunately, the largest isotope effect we might have observed, namely, ${}^Dk_{burst} = 4.09$, could not be accurately determined due to the very high K_{xylose} value.

Comparison of Cys298-Modified Enzyme Forms. Using the same type of analysis allows us to draw some interesting conclusions regarding the various Cys298-modified enzyme forms, namely, C298A, C298S, and "oxidized" human aldose reductase. The basic assumption is that the $V_{aldehyde}/E_t$ value is largely controlled by k_{11}. If that were not the case, and the k_7/k_{11} ratio were to change such that k_7 became a substantial contributor to the overall rate limitation for the reaction, we should see a significant increase in ${}^DV_{aldehyde}$. For example, the Y48H mutant hAR shows large and equivalent isotope effects on both $V_{aldehyde}/E_t$ and $V/K_{aldehyde}E_t$, consistent with the sequence of steps containing the hydride transfer being rate-limiting for the reduction reaction at all concentrations of aldehyde (Bohren et al., 1994). Since we have already determined that neither the oxidized hAR enzyme form nor the C298S mutant shows any large ${}^DV_{aldehyde}$ (Grimshaw and Lai, unpublished results), this assumption appears to be valid. Thus, because $K_{aldehyde} \cong k_{11}/k_5$, the apparent $K_{aldehyde}$ will directly reflect changes in both k_{11} and k_5. Changes in $V_{aldehyde}/E_t$, on the other hand, relate only to changes in k_{11}, and therefore changes in $V/K_{aldehyde}E_t$ give the effect on k_5 directly, since $V/K_{aldehyde}E_t$ is merely the ratio of the other two kinetic parameters.

Table 5 lists a comparison of compiled data for the relative change in the observable kinetic parameters $V_{aldehyde}/E_t$ and $K_{aldehyde}$ for C298A, C298S, and "oxidized" hAR relative to the values for wild-type enzyme. The trend in the parameter values is clear—all of the enzymes display roughly the same increase in K_m for DL-glyceraldehyde, but the relative increase in $V_{aldehyde}/E_t$ value ranges from a maximum of almost 9-fold for C298A, to 3.5-fold for C298S, and finally no change for oxidized hAR. By the above reasoning, the contribution of k_{11} must decrease in the same order, while the contribution of k_5, or the sequence of steps which comprises k_5, must *increase* going from C298A to C298S, and finally to oxidized hAR. The decrease in k_5 value, which reflects binding of the aldehyde substrate to the *E·NADPH complex, is paralleled by the increase in K_i value for sorbinil, a potent ARI for the wild-type enzyme which binds preferentially to the *E·NADP$^+$ complex (Liu et al., 1992b; Ward et al., 1993; Ehrig et al., 1994).

In terms of the enzyme structure, the trend in k_{11} and k_5 values for the various enzyme forms suggests that removing the -SH moiety from wild-type enzyme to yield the Ala298 mutant enzyme has a greater effect on the conformational change, but a smaller effect on aldehyde or ARI binding. Substitution of the -SH moiety by an -OH group has the opposite effect. Thus, in the C298A mutant the conformational change shows a small effect, and the large effect is seen for aldehyde and ARI binding. Finally, for oxidized hAR, which the studies of Mura and co-workers (Del Corso et al., 1989, 1993; Giannessi et al., 1993; Cappiello et al., 1994) suggest may consist of a mixed disulfide between Cys298 and an organic thiol such as cysteine or glutathione, there is apparently no effect on k_{11}, but the binding of either DL-glyceraldehyde or Sorbinil is drastically worsened. The latter result suggests that a mixed disulfide formed at the Cys298 position may be able to interact directly with the active site in such a way that the closed conformation of the nucleotide enfolding loop is stabilized, but the binding of aldehyde or ARI in the catalytic site is essentially blocked. Furthermore, the net effect on $V_{aldehyde}/E_t$ depends on the nature of the organic thiol used to generate the mixed disulfide with AR; neutral thiols such as 2-mercaptoethanol yield an increase in turnover number, while zwitterionic thiols such as glutathione or cysteine result in a decrease in $V_{aldehyde}/E_t$ (Cappiello et al., 1994). It will be interesting to see if these turnover numbers truly reflect the k_{11} values for the various mixed disulfide forms of AR.

It has been proposed (Ward et al., 1993) that the decrease in ARI potency seen for the oxidized or "ARI-insensitive" form of AR could be explained by a decrease in the steady-state concentration of the *E·NADP$^+$ complex that binds ARIs due to an increase in the forward isomerization rate constant (k_{11} in Scheme 1). However, in order to account for the observed 10- to 1000-fold increase in the K_i value (Table 4) by this mechanism, the steady-state concentration of *E·NADP$^+$ would have to decrease from the $0.99E_t$ level established for the wild-type enzyme (Grimshaw et al., 1995a) to roughly $(0.10-0.01)E_t$, respectively. For the C298A mutant enzyme, which shows about the same K_i value for Sorbinil as wild-type enzyme, we can calculate from the rate constants in Table 3 that *E·NADP$^+$ will comprise 97% of E_t during the steady-state reduction reaction at a saturating level of D-xylose, which is only 2% less than for wild-type enzyme. Similarly, for the C298S mutant enzyme, for which we have argued above that k_{11} must be faster than wild-type but slower than the C298A mutant enzyme, the steady-state level of *E·NADP$^+$ will be similar. Thus, the 10-fold increase in K_i for Sorbinil cannot be explained solely by an effect on k_{11}. A similar argument can be made for the oxidized enzyme form where $V_{aldehyde}/E_t$ (and thus the steady-state level of *E·NADP$^+$) is the same as wild-type, but the K_i Sorbinil value has increased 1000-fold. The large increase in K_i value for most but not all (Grimshaw et al., 1989;

Bhatnagar et al., 1989, 1994; Petrash et al., 1992, 1993; Bohren & Gabbay, 1993; Vander Jagt & Hunsaker, 1993) ARIs as inhibitors of the C298S and oxidized hAR enzymes must therefore be due to steric or other effects occurring at the active site.

These studies demonstrate the usefulness of combining steady-state, pre-steady-state, and isotope effect measurements to localize the subtle kinetic effects observed in a mutant enzyme within the particular steps in the overall reaction mechanism. The dominant effect observed for the C298A mutant enzyme is ascribed to an increase in the rate of opening of the nucleotide-enfolding loop which precedes nucleotide exchange, with lesser effects on the rates for aldehyde binding and subsequent hydride transfer. The elevated V/E_t and K_m values for C298A reveal this mutant to be ideally suited to the type of pH studies described in the succeeding paper where the important role of Tyr48, the active site acid−base residue integrally involved in catalysis and inhibitor binding, is further clarified. The changes in specific steps affect many of the observable kinetic parameters, and it is only through the use of the complete kinetic model that it has been possible to confidently interpret these subtle changes in the context of individual rate constants within the overall reaction mechanism.

ACKNOWLEDGMENT

The authors thank Dr. Bryce V. Plapp and the members of his laboratory at the University of Iowa, in particular Dr. Keehyuk Kim, for the use of the stopped-flow instrument and for many helpful discussions.

REFERENCES

Bhatnagar, A., Liu, S.-Q., Das, B., & Srivastava, D. K. (1989) *Mol. Pharmacol. 36*, 825−830.

Bhatnagar, A., Liu, S.-Q., Ueno, N., Chakrabarti, B., & Srivastava, S. K. (1994) *Biochim. Biophys. Acta 1205*, 207−214.

Bohren, K. M., & Gabbay, K. H. (1993) in *Enzymology and Molecular Biology of Carbonyl Metabolism 4* (Weiner, H., Ed.) pp 267−277, Plenum Press, New York.

Bohren, K. M., Page, J. L., Shankar, R., Henry, S. P., & Gabbay, K. H. (1991) *J. Biol. Chem. 266*, 24031−24037.

Bohren, K. M., Grimshaw, C. E., Lai, C.-J., Harrison, D. A., Ringe, D., Petsko, G. A., & Gabbay, K. H. (1994) *Biochemistry 33*, 2021−2032.

Borhani, D. W., Harter, T. M., & Petrash J. M. (1992) *J. Biol. Chem. 267*, 24841−24847.

Bruce, N. C., Willey, D. L., Coulson, A. F. W., & Jeffery, J. (1994) *Biochem. J. 299*, 805−811.

Cappiello, M., Voltarelli, M., Giannessi, M., Cecconi, I., Camici, G., Manao, G., Del Corso, A., & Mura, U. (1994) *Exp. Eye Res. 58*, 491−501.

Clarke, A. R., Widley, D. B., Chia, W. N., Barstow, D., Atkinson, T., & Holbrook, J. J. (1896) *Nature (London) 324*, 699−702.

Cleland, W. W. (1975) *Biochemistry 14*, 3220−3224.

Cleland, W. W. (1977) *Adv. Enzymol. Relat. Areas Mol. Biol. 45*, 273−388.

Cleland, W. W. (1987) in *Isotopes in Organic Chemistry* (Buncel, E., & Lee, C. C., Eds.) Vol. 7, Chapter 2, Elsevier, Amsterdam.

Cook, P. F., Blanchard, J. S., & Cleland, W. W. (1980) *Biochemistry 19*, 4853−4858.

Del Corso, A., Barsacchi, D., Giannessi, M., Tozzi, M. G., Camici, M., & Mura, U. (1989) *J. Biol. Chem. 264*, 17653−17655.

Del Corso, A., Valtarelli, M., Giannessi, M., Cappiello, M., Barsacchi, D., Zandomeneghi, M., Camici, M., & Mura, U. (1993) *Arch. Biochem. Biophys. 300*, 430−433.

Ehrig, T., Bohren, K. M., Prendergast, F. G., & Gabbay, K. H. (1994) *Biochemistry 33*, 7157−7165.

Fersht, A. R. (1988) *Biochemistry 27*, 1577−1580.

Giannessi, M., Del Corso, A., Cappiello, M., Voltarelli, M., Marini, I., Barsacchi, D., Garland, D., Camici, M., & Mura, U. (1993) *Arch. Biochem. Biophys. 300*, 423−429.

Grimshaw, C. E. (1992) *Biochemistry 31*, 10139−10145.

Grimshaw, C. E., & Lai, C.-J. (1995) *Arch. Biochem. Biophys.* (submitted).

Grimshaw, C. E., Shahbaz, M., Jahangiri, G., Putney, C. G., McKercher, S. R., & Mathur, E. J. (1989) *Biochemistry 28*, 5343−5353.

Grimshaw, C. E., Bohren, K. M., Lai, C.-J., & Gabbay, K. H. (1995a) *Biochemistry 34*, 14356−14365.

Grimshaw, C. E., Bohren, K. M., Lai, C.-J., & Gabbay, K. H. (1995b) *Biochemistry 34*, 14374−14384.

Harrison, D. H., Bohren, K. M., Ringe, D., Petsko, G. A., & Gabbay, K. H. (1994) *Biochemistry 33*, 2011−2020.

Hayward, L. D., & Angyal, S. J. (1977) *Carbohydr. Res. 53*, 13−20.

Hermes, J. D., Roeske, C. A., O'Leary, M. H., & Cleland, W. W. (1982) *Biochemistry 21*, 5106−5114.

Kador, P. F., Shiono, T., & Kinoshita, J. H. (1983) *Invest. Ophthalmol. Visual Sci. 24*, 267 (Suppl.).

Kormann, A. W., Hurst, R. O., & Flynn, T. G. (1972) *Biochim. Biophys. Acta 258*, 4055.

Kubiseski, T. J., Hyndman, D. J., Morjana, N. A., & Flynn, T. G. (1992) *J. Biol. Chem. 267*, 6510−6517.

Liu, S.-Q., Bhatnagar, A., Das, B., & Srivastava, S. K. (1989) *Arch. Biochem. Biophys. 275*, 112−121.

Liu, S.-Q., Bhatnagar, A., & Srivastava, S. K. (1992a) *Biochim. Biophys. Acta 1120*, 329−336.

Liu, S.-Q., Bhatnagar, A., & Srivastava, S. K. (1992b) *Biochem. Pharmacol. 44*, 2427−2429.

Moonsammy, G. I., & Stewart, M. A. (1961) *J. Neurochem. 14*, 1187−1193.

Northrop, D. B. (1977) in *Isotope Effects on Enzyme-Catalyzed Reactions* (Cleland, W. W., O'Leary, M. H., & Northrop, D. B., Eds.) pp 122−152, University Park Press, Baltimore.

Petrash, J. M., Harter, T. M., Devine, C. S., Olins, P. O., Bhatanagar, A., Liu, S.-Q., & Srivastava, S. K. (1992) *J. Biol Chem. 267*, 24833−24840.

Petrash, J. M., Harter, T., Tarle, I., & Borhani, D. (1993) in *Enzmology and Molecular Biology of Carbonyl Metabolism 4* (Weiner, H., Ed.) pp 289−300, Plenum Press, New York.

Qin, K., & Cheng, K.-C. (1994) *Biochemistry 33*, 3223−3228.

Rondeau, J.-M., Tête-Favier, F., Podjarny, A., Reymann, J.-M., Barth, P., Biellmann, J.-F., & Moras, D. (1992) *Nature 355*, 469−472.

Scharschmidt, M., Fisher, M. A., & Cleland, W. W. (1984) *Biochemistry* 23, 5471−5478.

Tarle, I., Borhani, D. W., Wilson, D. K., Quiocho, F. A., & Petrash, J. M. (1993) *J. Biol. Chem. 268*, 25687−25693.

Vander Jagt, D. L., & Hunsaker, L. A. (1993) *Enzymology and Molecular Biology of Carbonyl Metabolism 4* (Weiner, H., Ed.) pp 279−288, Plenum Press, New York.

Vander Jagt, D. L., Stangbeye, D. K., Hunsaker, L. A., Eaton, R. P., & Sibbit, W. L., Jr. (1988) *Biochem. Pharmacol. 37*, 1051−1056.

Vander Jagt, D. L., Robinson, B., Taylor, K. K., & Hunsaker, L. A. (1990) *J. Biol. Chem. 265*, 20982−20987.

Ward, W. H. J., Cook, P. N., Mirrlees, D. J., Brittain, D. R., Preston, D. J., Carey, F., Tuffin, D. P., & Howe, R. (1993) *Enzymology and Molecular Biology of Carbonyl Metabolism 4* (Weiner, H., Ed.) pp 310−321, Plenum Press, New York.

Wilson, D. K., Bohren, K. M., Gabbay, K. H., & Quiocho, F. A. (1992) *Science 251*, 81−84.

Wilson, D. K., Tarle, I., Petrash, J. M., & Quiocho, F. A. (1993) *Proc. Natl. Acad. Sci. USA 90*, 9847−9851.

BI950556C